PHYSICAL REVIEW D **85,** 054002 (2012)

Top quark pair production in association with a jet: QCD corrections and jet radiation in top quark decays

Kirill Melnikov,[1] Andreas Scharf,[2,3] and Markus Schulze[1,4]

[1]*Department of Physics and Astronomy, Johns Hopkins University, Baltimore, Maryland, USA*
[2]*Department of Physics, State University of New York at Buffalo, Buffalo, New York, USA*
[3]*Institute for Theoretical Physics and Astrophysics, University of Würzburg, Würzburg, Germany*
[4]*High Energy Physics Division, Argonne National Laboratory, Argonne, Illinois 60439, USA*

(Received 2 December 2011; published 1 March 2012)

We consider top quark pair production in association with a hard jet through next-to-leading order in perturbative QCD. Top quark decays are treated in the narrow width approximation and spin correlations are retained throughout the computation. We include hard jet radiation by top quark decay products and explore their importance for basic kinematic distributions at the Tevatron and the LHC. Our results suggest that QCD corrections and jet radiation in decays can lead to significant changes in shapes of basic distributions and, therefore, need to be included for the description of $t\bar{t}j$ production.

DOI: 10.1103/PhysRevD.85.054002 PACS numbers: 14.65.Ha

I. INTRODUCTION

Experiments at the LHC are in the process of accumulating a large data set of top quark pairs that will allow detailed studies of various processes that Tevatron experiments either observed with relatively low statistics or did not observe at all. Such processes include associated production of a $t\bar{t}$ pair with a jet [1], a photon [2], two jets, a Z boson, or a Higgs boson. Beyond studies of $t\bar{t}$ pair production at very high invariant masses, detailed investigations of associated production processes will mark the beginning of the post-Tevatron era in top quark physics. A significant body of theoretical work is devoted to improving predictions for $t\bar{t}$ associated production processes (see Refs. [3–12]).

It is well-known that, once produced, top quarks decay very rapidly. For this reason top quarks are observed and studied indirectly through kinematic features of their decay products. Unfortunately, this complicates top quark studies by introducing additional uncertainties in kinematic reconstructions due to finite resolution on energies and angles of decay products, missing energy, as well as backgrounds, including combinatorial ones. On the positive side, the rapid decay of top quarks enables the description of their decay products in perturbative QCD without the need to resort to fragmentation functions and other nonperturbative objects.

A precise description of hard hadron collisions requires the application of perturbative QCD through next-to-leading order (NLO) in the expansion of the strong coupling constant. The complete NLO QCD description of any process that involves $t\bar{t}$ production should include QCD corrections to top quark pair production and to top quark decays. For processes where top quarks are produced in association with a photon or a jet, a standard process to study is $t\bar{t}X$ production with $X = \gamma, j$, followed by the top quark decay $t \to bW$. However, since both photons and jets can be radiated in top quark decays, one should also consider $t\bar{t}$ production followed by ''radiative'' decays, such as $t \to bWj$ and $t \to bW\gamma$. The importance of radiation in the decays strongly depends on the selection criteria that are used to isolate a particular process and, hence, cannot be quantified *a priori*. For example, in a recent measurement of $t\bar{t}\gamma$ production by the CDF Collaboration [2], about half of all signal events come from the process $p\bar{p} \to t\bar{t}$ followed by the radiative decay of the top quark $t \to Wb\gamma$ [9]. To compare its measurement with theoretical predictions, CDF uses a NLO QCD K factor for the process $p\bar{p} \to t\bar{t}\gamma$ computed with stable top quarks. However, since about half of CDF's events come from $t\bar{t}$ production followed by radiative decays of top quarks, it is unclear if such a comparison is meaningful.

In principle, one can get around the problem of separating production and decay stage by simply giving up on the approximation that top quarks are produced on-shell and focusing instead on the fully realistic final state such as $b\bar{b}W^+W^-X$ with $X = \gamma, j, jj, H, Z$. A calculation of $pp \to b\bar{b}W^+W^-X$ through a given order in the perturbative expansion in QCD leads to a prediction for a final state that includes both ''resonant'' and ''nonresonant'' contributions, providing a complete description of the process. Without a doubt, this is the best approach possible, provided that it is feasible. The feasibility depends on the approximation in perturbative QCD at which the process of interest is considered. At leading order, this approach can be pursued for an essentially arbitrarily complicated process thanks to automated programs such as MADGRAPH [13]. However, this approach becomes very complex already at NLO QCD. For the simplest process $pp \to W^+W^-b\bar{b}$ that, among many other ways, can occur through the production of a nearly on-shell $t\bar{t}$ pair, this was recently accomplished in Refs. [14,15]. Applications of this approach to more complicated processes are

difficult to imagine. On the contrary, a sequential treatment of various production and decay stages based on the double resonant approximation for t and $\bar{t}$ can be generalized to processes of significant complexity, at least as a matter of principle. This double resonance approximation is parametrically controlled by the ratio of the top quark width to its mass $\Gamma_t/m_t \sim 10^{-2}$ and should be sufficiently accurate for most observables. In fact, there has been significant progress in using this approximation to describe top quark pair production recently. For example, $t\bar{t}$ pair production at NLO QCD in the double resonance approximation, including corrections to top quark decays and spin correlations, was computed in Refs. [16–23]. The number of similar computations for more complicated processes is rather limited. The only process for which a full description is available is associated production of $t\bar{t}\gamma$ [9], where NLO QCD corrections to the production and decays, including the radiative one ($t \to Wb\gamma$), are computed.

The production of $t\bar{t}j$ at NLO QCD was first studied in Refs. [24,25] for stable top quarks and later in Ref. [26] where decays were included at leading order. A different approach to this process is described in Refs. [27,28], where $t\bar{t}j$ production at NLO QCD is combined with a parton shower, following the POWHEG procedure [29]. Top quark decays are treated in the parton shower approximation where $t\bar{t}$ spin correlations are omitted either at leading [27] or at next-to-leading [28] order, and whose correspondence with NLO QCD computations is not clear.

Fortunately, these approximations are not necessary, since it is possible to treat the complete process $t\bar{t}j \to b\bar{b}W^+W^-j$ in the narrow width approximation where top quark decays, including $t \to Wbj$, are described consistently at NLO QCD and spin correlations are retained throughout the entire decay chain. Such a calculation gives a state-of-the-art description of the $t\bar{t}j$ production that, in principle, can be directly compared to experimental results as theoretical predictions for a complete and fully realistic final state become available. The goal of the present paper is therefore to extend the description of $pp \to t\bar{t}j$ production given in Ref. [26] by including radiation in the decay through next-to-leading order in perturbative QCD.

The paper is organized as follows. In the next section, we outline the framework of our calculation and discuss technical aspects of the computation which arise because of the need to treat radiative corrections to processes with decay kinematics. Phenomenological results for the Tevatron and the 7 TeV LHC are presented in Sec. III. We conclude in Sec. IV.

II. TECHNICAL ASPECTS OF THE CALCULATION

In this section, we summarize the technical aspects of the calculation. We begin by describing various contributions that we require for the computation. As we pointed out already, the top quark is treated in the narrow width approximation. This approximation is obtained from the full cross section with unstable top quarks by taking the limit $\Gamma_t \to 0$ and neglecting all terms that are less singular than Γ_t^{-2}. See Ref. [22] for further details. This allows us to organize the computation in terms of a production process which includes the hard collision, and the decay process. To give a complete list of all necessary contributions for $t\bar{t}$ + jet production calculation, we begin by writing the formula for the inclusive cross section as a convolution of the production cross section $\sigma_{t\bar{t}}$ and the decay rate Γ_t:

$$d\sigma_{\text{incl}} = \Gamma_{t,\text{tot}}^{-2}(d\sigma_{t\bar{t}+0j} + d\sigma_{t\bar{t}+1j} + d\sigma_{t\bar{t}+2j} + \cdots) \otimes (d\Gamma_{t\bar{t}+0j} + d\Gamma_{t\bar{t}+1j} + d\Gamma_{t\bar{t}+2j} + \cdots). \quad (1)$$

Subscripts denote the number of exclusive jets defined according to some jet algorithm. We further use the abbreviation $d\Gamma_{t\bar{t}+nj} = \sum_{l=0}^{n} d\Gamma_{t+lj} d\Gamma_{\bar{t}+(n-l)j}$ to summarize the decay rates of the top and antitop quark in association with a fixed number of jets.

We can now expand Eq. (1) assuming that the number of jets that we eventually require is equal or larger than 1 and that the cross sections and widths for each jet multiplicity scale as $\sigma_{t\bar{t},nj} \sim \mathcal{O}(\alpha_s^{2+n})$ and $\Gamma_{t,nj} \sim \mathcal{O}(\alpha_s^n)$. Since we are interested in NLO QCD corrections to one-jet production, we can disregard all terms that depend on powers of α_s higher than four. We obtain

$$d\sigma_{t\bar{t}+1j}^{\text{NLO}} = \Gamma_{t,\text{tot}}^{-2}(d\sigma_{t\bar{t}+0j} d\Gamma_{t\bar{t}+1j} + d\sigma_{t\bar{t}+0j} d\Gamma_{t\bar{t}+2j} + d\sigma_{t\bar{t}+1j} d\Gamma_{t\bar{t}+0j} + d\sigma_{t\bar{t}+1j} d\Gamma_{t\bar{t}+1j} + d\sigma_{t\bar{t}+2j} d\Gamma_{t\bar{t}+0j}), \quad (2)$$

and we rewrite this formula in a way that separates various processes that contribute to the cross section:

$$d\sigma_{t\bar{t}+1j}^{\text{NLO}} = \Gamma_{t,\text{tot}}^{-2}(d\sigma_{t\bar{t}+1j}^{\text{LO}} d\Gamma_{t\bar{t}+1j}^{\text{LO}} + d\sigma_{t\bar{t}}^{\text{LO}} d\Gamma_{t\bar{t}+1j}^{\text{LO}} + \overbrace{(d\sigma_{t\bar{t}+1j}^{\text{virt}} + d\sigma_{t\bar{t}+2j}^{\text{real}}) d\Gamma_{t\bar{t}}^{\text{LO}}}^{\text{(a)}} + \overbrace{d\sigma_{t\bar{t}}^{\text{LO}} (d\Gamma_{t\bar{t}+1j}^{\text{virt}} + d\Gamma_{t\bar{t}+2j}^{\text{real}})}^{\text{(b)}} + \underbrace{d\sigma_{t\bar{t}+1j}^{\text{real}} d\Gamma_{t\bar{t}+1j}^{\text{real}} + d\sigma_{t\bar{t}}^{\text{virt}} d\Gamma_{t\bar{t}+1j}^{\text{LO}} + d\sigma_{t\bar{t}+1j}^{\text{LO}} d\Gamma_{t\bar{t}}^{\text{virt}}}_{\text{(c)}}). \quad (3)$$

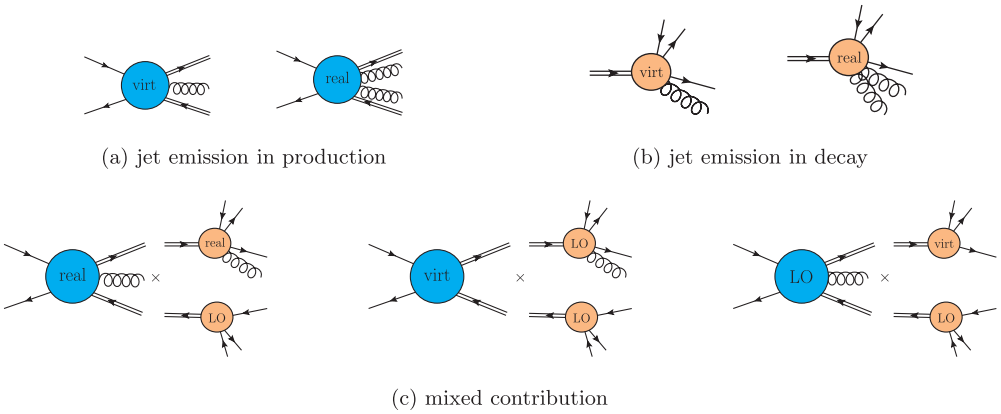

(a) jet emission in production (b) jet emission in decay

(c) mixed contribution

FIG. 1 (color online). NLO QCD corrections to top quark pair production and decay in association with a jet. Contributions (a) and (b) show jet emission in production and decay, respectively. The symbol "real" indicates that one parton is allowed to be unresolved. (c) defines the "mixed" contributions.

We now review different contributions that appear in Eq. (3). The first and second terms describe $t\bar{t}+j$ production at leading order followed by leading order decays of the top quark and $t\bar{t}$ production followed by a radiative decay of the top quark, respectively. The third and forth terms represent the NLO QCD corrections to the production process $t\bar{t}+j$, where the symbol "real" indicates that one parton is allowed to become unresolved. The last two terms in the first line of Eq. (3) describe leading order production of a top quark pair followed by NLO QCD corrections to the "radiative decay" $t \to W+b+j$.[1] Finally, the terms in the second line of Eq. (3) describe mixed contributions where jet emission occurs simultaneously in both production and decay stage. Since one of those jets can be unresolved, the last two terms are the corresponding virtual corrections needed to provide an infrared finite result. In the remainder of the paper we will refer to contribution (a) and (b) in Eq. (3) as jet radiation in the production and jet radiation in the decay, respectively. The last part (c) we call the mixed contribution. The corresponding topologies are depicted in Fig. 1.

Let us now describe how NLO QCD corrections to jet radiation in the production processes $pp \to t\bar{t}$ and $pp \to t\bar{t}j$ are treated. We note that—when production processes are considered at next-to-leading order—the decay processes are included at leading order, consistent with the expansion in α_s. However, these leading order decays are different processes: in the former case, we consider the radiative decay $t \to Wbg$, since an additional jet is required in the final state. In the latter case, top quarks decay into the Wb final state since the jet is created in the production stage. The NLO QCD results for the production processes are available; they are described in Refs. [22,26] including an efficient way of implementing the decays of top quarks while retaining all spin correlations. We note that one-loop QCD corrections to $0 \to q\bar{q}t\bar{t}$, $0 \to ggt\bar{t}$, $0 \to q\bar{q}t\bar{t}g$, and $0 \to gggt\bar{t}$ amplitudes that we require are calculated using generalized D-dimensional unitarity [30–32]. The real emission corrections are obtained following the Catani-Seymour dipole subtraction formalism [33] and its extension to massive particles in Ref. [34]. To improve the efficiency of the computation, we follow Ref. [35] and use α parameters to restrict subtraction terms to singular phase-space regions. The relevant dipoles with α parameters are found in Refs. [12,36,37].

The second part required in the calculation involves leading order production processes $pp \to t\bar{t}$ and $pp \to t\bar{t}j$ followed by top quark decays at next-to-leading order. In the former case the NLO QCD corrections to radiative decays $t \to Wbj$ and $W \to q\bar{q}g$ are required; in the latter case $t \to Wb$ and $W \to q\bar{q}$ need to be computed through NLO QCD. Radiative corrections to $t \to Wb$ and $W \to q\bar{q}$ are known; our implementation follows the description in Ref. [22]. We do not repeat it here and focus, instead, on the NLO QCD corrections to the "radiative decay" $t \to bWj$. Since this is a sufficiently low-multiplicity process, we compute the virtual corrections using Passarino-Veltman reduction of tensor integrals [38]. The scalar integrals are taken from Ref. [39]. For the calculation of the real corrections we need to consider various decay processes, such as $t \to (W \to q\bar{q}')bgg$, $t \to (W \to q\bar{q}'gg)b$, $t \to (W \to q\bar{q}'g)bg$, etc. The real emission subtraction terms are again constructed using the dipole formalism of Catani and Seymour [33]. However, we note that its application to decay processes requires clarification. Catani and Seymour constructed subtraction terms—the dipoles—that satisfy two criteria: (1) they remove infrared and collinear singularities when subtracted from scattering amplitudes and (2) they can be integrated analytically over the unresolved phase space. In the original paper [33], it is shown how to satisfy these conditions for two colliding massless

[1]We note that, in the case of a semileptonic top quark decay, also the W boson is allowed to radiate an additional hard jet at NLO QCD. We include this contribution in our computation as well.

partons. Since decay kinematics differ from production kinematics, some of the Catani-Seymour dipoles need to be modified if we deal with decays of color-charged particles.

Recall that within the Catani-Seymour dipole formalism, dipoles are constructed by taking different partons to be ''emitters'' and ''spectators,'' in addition to soft or collinear partons that are actually ''emitted.'' The dipoles depend on ''flavors'' (quarks, gluons) of emitted and emitters and on whether emitters and spectators are in the initial or in the final state. The corresponding dipoles are referred to as final-final, final-initial, initial-initial, and initial-final.

However, only a limited number of these dipoles are needed for the decay processes in general. First, it is obvious that there are no initial-initial dipoles since there is just one particle in the initial state. Final-final dipoles can be borrowed from Ref. [33] and the phase-space remapping therein. Initial-final dipoles can be omitted since real radiation by a massive initial state particle is only singular in soft kinematics. This contribution can be absorbed into final-initial dipoles which are the only dipoles for decay kinematics that need to be constructed.

The complete list of dipoles that we need for the process $t \to W b g_1 g_2$ is $\mathcal{D}_{g_1 g_2, b}$, $\mathcal{D}_{b g_1, g_2}$, $\mathcal{D}_{b g_2, g_1}$, $\mathcal{D}^t_{b g_1}$, $\mathcal{D}^t_{b g_2}$, and $\mathcal{D}^t_{g_1 g_2}$. The first three dipoles are of the final-final type whereas the last three dipoles are the missing final-initial dipoles. We will discuss their construction in the following. We need to distinguish two types of final-initial dipoles which correspond to the splitting $q \to qg$ and $g \to gg$ with a top quark in the initial state being the spectator.

We begin our discussion with the gluon-quark dipole. It can be extracted from Ref. [40]. To this end, we consider the process $t \to W b g_1 g_2$ and imagine that gluon g_1 and the (massless) b quark become unresolved. The top quark in the initial state is the spectator. We combine the momenta of the W boson and the gluon g_2 into a new momentum $\tilde{p}_W = p_W + p_{g_2}$ and introduce a variable $r^2 = \tilde{p}_W^2/m_t^2$. The remaining momenta—whose scalar products lead to soft and collinear singularities—are parametrized using two variables z and y:

$$p_b p_{g_1} = \frac{m_t^2}{2}(1-r)^2 y, \qquad p_t p_{g_1} = \frac{m_t^2}{2}(1-r^2)(1-z). \tag{4}$$

With this parametrization, the final-initial gluon-quark dipole reads [40]

$$D^t_{g_1 b} = 4\pi\alpha_s \mu^{2\epsilon}\left[\frac{1}{p_b p_{g_1}}\left(\frac{2}{1-z} - 1 - z - y\epsilon(1-z)\right) - \frac{m_t^2}{(p_t p_{g_1})^2}\right]\delta_{\lambda\lambda'}, \tag{5}$$

where $\epsilon = (4-d)/2$ is the parameter of dimensional regularization, d is the number of space-time dimensions, and λ, λ' are quark helicity labels. We note that Eq. (5) gives the dipole in the conventional dimensional regularization (CDR) scheme; if the four-dimensional helicity scheme [41] is used, the term proportional to ϵ in Eq. (5) should be dropped.

In Ref. [9] we have integrated the dipole in Eq. (5) over the restricted unresolved phase space [35], drawing extensively from the results of Ref. [40]. We reproduce this result here for completeness. We consider the integration of the dipole in Eq. (5) over the unresolved restricted phase space:

$$\int [dg][1-\theta(1-\alpha-z)\theta(y-\alpha y_{\max})] D^t_{g_1 b} = \mathcal{N}\int_0^1 dz (r^2 + z(1-r^2))^{-\epsilon} \int_0^{y_{\max}} dy\, y^{-\epsilon}(y_{\max}-y)^{-\epsilon}[1-\theta(1-\alpha-z)\theta(y-\alpha y_{\max})] D^t_{g_1 b}. \tag{6}$$

where

$$y_{\max} = \frac{(1+r)^2 z(1-z)}{z + r^2(1-z)}, \qquad \mathcal{N} = \frac{(1-r)^2}{16\pi^2} m_t^{2-2\epsilon} \frac{(4\pi)^\epsilon}{\Gamma(1-\epsilon)}\left(\frac{1+r}{1-r}\right)^{2\epsilon}. \tag{7}$$

We find the following result in CDR:

$$\int [dg] D^t_{g_1 b}[1-\theta(1-\alpha-z)\theta(y-\alpha y_{\max})] = \frac{\alpha_s}{2\pi}\frac{(4\pi\mu^2)^\epsilon}{m_t^{2\epsilon}\Gamma(1-\epsilon)}\delta_{\lambda\lambda'}\left[\frac{1}{\epsilon^2} + \frac{1}{\epsilon}\left(\frac{5}{2} - 2\ln(r_1)\right) + \frac{27}{4} + \frac{1}{2}\left(\frac{1}{r_1^2} - \frac{8}{r_1} + 7\right)\ln r^2 + \frac{1}{2r_1} + 2\,\mathrm{Li}_2(r_1) - \frac{5\pi^2}{6} - 5\ln(r_1) + 2\ln^2(r_1) - 2\ln^2\alpha - \left(\frac{7}{2} - 4\alpha + \frac{\alpha^2}{2}\right)\ln\alpha + \frac{2(1-\alpha)r^2}{r_1}\ln\left(\frac{1-r_1}{1-\alpha r_1}\right)\right], \tag{8}$$

with $r_1 = 1 - r^2$.

It remains to construct the gluon-gluon dipole of the final-initial type for decay kinematics. In variance with the gluon-quark dipole just considered, the gluon-gluon dipole contains nontrivial spin correlations. We will use the parametrization of the unresolved phase space that we just discussed with an obvious modification of the momentum $\tilde{p}_W$; for the gluon-gluon dipole, it is given by $\tilde{p}_W = p_W + p_b$. To derive the gluon-gluon dipole, we consider the limit of the $0 \to \bar{t} b g_1 g_2 W$ amplitude squared when two gluons become collinear. The result reads

$$|\mathcal{M}|^2 \to \mathcal{M}^*_\mu P^{gg}_{\mu\nu} \mathcal{M}^\nu, \tag{9}$$

where

$$P^{gg}_{\mu\nu} \sim \Big[-g_{\mu\nu}\Big(\frac{\xi}{1-\xi} + \frac{1-\xi}{\xi}\Big) - 2(1-\epsilon)\xi(1-\xi)\frac{k^\mu_\perp k^\nu_\perp}{k^2_\perp}\Big] \tag{10}$$

is the spin-dependent splitting function. In Eq. (10), ξ and $k^\mu_\perp$ are defined as

$$\begin{aligned} p^\mu_{g_1} &= (1-\xi)p^\mu + k^\mu_\perp - \frac{k^2_\perp n^\nu}{(1-\xi)(2pn)}, \\ p^\mu_{g_2} &= \xi p^\mu - k^\mu_\perp - \frac{k^2_\perp n^\nu}{\xi(2pn)}, \end{aligned} \tag{11}$$

where the lightlike vector p defines the collinear direction and another lightlike vector n_μ is auxiliary. We can now use the relations between gluon momenta

$$\begin{aligned} k^\mu_\perp \approx a_\mu &= \xi p^\mu_{g_1} - (1-\xi)p^\mu_{g_2}, \\ 2p_{g_1}p_{g_2} &= -\frac{k^2_\perp}{\xi(1-\xi)}, \end{aligned} \tag{12}$$

to write

$$P^{gg}_{\mu\nu} \sim \Big[-g_{\mu\nu}\Big(\frac{\xi}{1-\xi} + \frac{1-\xi}{\xi}\Big) + (1-\epsilon)\frac{a_\mu a_\nu}{(p_{g_1}p_{g_2})}\Big]. \tag{13}$$

To construct the dipoles, we split this expression into two terms:

$$\frac{P^{gg}_{\mu\nu}}{2p_{g_1}p_{g_2}} \sim D^{1,2}_{\mu\nu} + D^{2,1}_{\mu\nu}, \tag{14}$$

where

$$D^{1,2}_{\mu\nu} = \frac{1}{2p_{g_1}p_{g_2}}\Big\{ -\frac{\xi g_{\mu\nu}}{(1-\xi)} + \frac{1-\epsilon}{2}\frac{a^\mu a^\nu}{(p_{g_1}p_{g_2})}\Big\} \tag{15}$$

and $D^{2,1}_{\mu\nu}$ is given by Eq. (15) with $\xi \to 1-\xi$. We would like to rewrite this equation in such a way that the integration over the unresolved phase space becomes straightforward. To this end, we express Eq. (15) in terms of the variables z and y and momentum of the top quark p_t and $\tilde{p}_W$. Because

$$\frac{(p_t p_{g_1})}{(p_t p_{g_2})} = \frac{1-\xi}{\xi}, \tag{16}$$

we can identify ξ with the variable z in Eq. (4). It remains to modify the spin-correlation part of Eq. (15) and write it in appropriate variables. We note that such modifications can be arbitrary provided that the original form of the spin-correlation part of the dipole is recovered in the limit when p_{g_1} and p_{g_2} become collinear. We do that by writing

$$a^\mu \to \pi^\mu = \Big(g^{\mu\nu} - \frac{p^\mu_t \tilde{p}^\nu_{12} + p^\nu_t \tilde{p}^\mu_{12}}{p_t \tilde{p}_{12}}\Big)a_\nu. \tag{17}$$

In Eq. (17), the momentum $\tilde{p}_{12}$ is the lightlike vector given by $\tilde{p}_{12} = p_t - \Lambda\tilde{p}_W$, where Λ is the Lorentz transformation constructed explicitly in Ref. [40]. The reduced matrix element that describes the decay process $t \to W + b + g$ is then evaluated for p_t, $\Lambda\tilde{p}_W$, and $\tilde{p}_{12}$, where $\Lambda\tilde{p}_W$ is then split into the W momentum and the b-quark momentum. We note that the projection operator introduced in Eq. (17) ensures that π_μ is transverse to $\tilde{p}_{12}$. As we show below, this feature simplifies the integration over the unresolved phase space considerably. It is straightforward to check that in the collinear ($y \to 0$) limit, $\pi_\mu \to a_\mu$. Hence, to construct a suitable dipole, we can simply substitute π_μ for a_μ in Eq. (15). Note also that we are allowed to multiply the spin-correlation part in Eq. (15) by an arbitrary function $f(y, z)$ provided that it is free of singularities and that it is normalized in such a way that $f(0, z) = 1$. We choose this function to be

$$f(y,z) = \frac{4}{m^4_t}\frac{(p_t\tilde{p}_W)^2 - r^2 m^4_t}{(1-r^2)^2}, \tag{18}$$

to simplify the calculation of the integrated dipole with α dependence. As the very last step, we add one more term to the dipole, to account for soft singularities that appear when a gluon is emitted from the top quark in the initial state. We are finally in the position to write down the gg final-initial dipole. In the CDR scheme, the result reads

$$D^{\mu\nu,t}_{g_1,g_2} = 4\pi\alpha_s\mu^{2\epsilon}\frac{1}{2p_{g_1}p_{g_2}}\Big[-g^{\mu\nu}\Big(\frac{z}{1-z} - \frac{m^2_t}{4}\frac{2p_{g_1}p_{g_2}}{(p_t p_{g_1})^2}\Big) + \frac{(1-\epsilon)\pi^\mu\pi^\nu}{2p_{g_1}p_{g_2}} f(y,z)\Big]. \tag{19}$$

The various quantities that appear in Eq. (19) are

$$\begin{aligned}
\pi^\mu &= \frac{1}{p_t\tilde{p}_{12}}((p_t\tilde{p}_{12})a^\mu - p_t^\mu(\tilde{p}_{12}a)),\\
a^\mu &= \frac{2}{m_t^2(1-r^2)}[(p_t p_{g_2})p_{g_1}^\mu - (p_t p_{g_1})p_{g_2}^\mu],\\
p_t p_{g_1} &= \frac{m_t^2}{2}(1-r^2)(1-z),\\
p_{g_1}p_{g_2} &= \frac{m_t^2}{2}(1-r)^2 y,\\
p_t\tilde{p}_{12} &= \frac{m_t^2(1-r^2)}{2},
\end{aligned} \tag{20}$$

with $r^2 = (p_W + p_b)^2/m_t^2$.

To integrate the dipole in Eq. (19) over the unresolved phase space, we make use of the results presented in Ref. [40]. It is straightforward to integrate the part proportional to the metric tensor. Integration of the spin-correlation part is more involved but it can be simplified because vector π^μ is orthogonal to the lightlike vector $\tilde{p}_{12}^\mu$. This allows us to write

$$\left\langle \frac{\pi^\mu\pi^\nu}{(2p_1p_2)^2}\right\rangle_{y,z} = A_1\left(-g^{\mu\nu} + \frac{p_t^\mu\tilde{p}_{12}^\nu + \tilde{p}_{12}^\mu p_t^\nu}{p_t\tilde{p}_{12}}\right) + A_2\tilde{p}_{12}^\mu\tilde{p}_{12}^\nu, \tag{21}$$

where $\langle\cdots\rangle_{y,z}$ denotes the integration over y and z as in Eq. (6). The term proportional to A_2 can be dropped since it gets Lorentz-contracted with the product of on-shell matrix elements that vanish when contracted with $\tilde{p}_{12}$. Hence, we only need to compute A_1, which we easily obtain by contracting the left-hand side of the above formula with the metric tensor. By the same argument, once A_1 is obtained, we can drop terms proportional to $\tilde{p}_{12}^\mu$ in tensorial structure that is multiplied by A_1 in Eq. (21). Therefore, we can write the result of the integration of $D_{g_1,g_2}^{\mu\nu,t}$ over unresolved phase space as proportional to the metric tensor.

We now present the result for the integrated final-initial gg dipole in the CDR scheme for decay kinematics, including its full α dependence. The integrated dipole reads

$$\begin{aligned}
&\int [dg] D_{g_1g_2}^{\mu\nu,t}[1-\theta(1-\alpha-z)\theta(y-\alpha y_{\max})]\\
&= \frac{\alpha_s}{2\pi}\frac{(4\pi\mu^2)^\epsilon}{m_t^{2\epsilon}\Gamma(1-\epsilon)}g_{\mu\nu}\Bigg[\frac{1}{2\epsilon^2} + \frac{17-12\log r_1}{12\epsilon} - \frac{5\pi^2}{12} - \log^2\alpha - \frac{(1-\alpha)(23-\alpha+2\alpha^2)}{12}\log\alpha + \log^2 r_1\\
&\quad - \frac{17}{6}\log r_1 - \frac{r^2\log r}{6r_1^5}[6\alpha^3(1-r_1)(-2+r_1) - 3\alpha^2(1-r_1)(-6+5r_1) + 12\alpha r_1(r^2+r_1^3) + r_1^2(2+r_1(-1+11r_1))]\\
&\quad + \frac{(1-\alpha)r^2\log(1-\alpha r_1)}{4r_1^5}[(-2\alpha^2(1-r_1)(-2+r_1) + \alpha(-2+(5-3r_1)r_1) - 2 + r_1 + r_1^2 - 4r_1^4)]\\
&\quad + \mathrm{Li}_2(r_1) - \frac{1}{240r_1^4(1-\alpha r_1)}[-8\alpha^9 r_1^5 - 6\alpha^8 r_1^4(2-7r_1) - \alpha^7 r_1^3(20-68r_1+115r_1^2)\\
&\quad + \alpha^6 r_1^2(-40+130r_1-165r_1^2+216r_1^3) - \alpha^5 r_1(120-360r_1+410r_1^2-234r_1^3+305r_1^4)\\
&\quad + \alpha^4(240-180r_1-510r_1^2+650r_1^3-195r_1^4+278r_1^5) - \alpha^3(600-1140r_1+280r_1^2+460r_1^2-92r_1^4+97r_1^5)\\
&\quad + \alpha^2(360-1140r_1+900r_1^2+50r_1^3-63r_1^4-40r_1^5) + 10\alpha(12+6r_1-36r_1^2+10r_1^3+8r_1^4+91r_1^5)\\
&\quad + 10r_1^2(4r^2-91r_1^2)]\Bigg].
\end{aligned} \tag{22}$$

The integrated dipole given in Eq. (22) is the final ingredient we need to treat the real emission contributions to radiative decays of top quarks.

III. PHENOMENOLOGICAL RESULTS

In this section we present phenomenological results for the Tevatron ($\sqrt{s} = 1.96$ TeV) and the LHC ($\sqrt{s} = 7$ TeV). We choose $m_t = 172$ GeV for the top quark mass and $m_W = 80.419$ GeV for the W-boson mass. We employ MSTW2008 parton distribution functions [42] and use the corresponding values of α_s at leading and next-to-leading order. The couplings of the W boson to fermions are obtained from the Fermi constant $G_F = 1.166\,39 \times 10^{-5}$ GeV^{-2}. Since we work in the narrow width approximation, our results are inversely proportional to the top quark and the W-boson widths, $\sigma \sim \Gamma_t^{-2}\Gamma_W^{-2}$. These decay widths are evaluated at leading and next-to-leading order in the strong coupling constant, for LO and NLO cross sections, respectively. For reference, we give the results for the widths:

$$\begin{aligned}
\Gamma_t^{\mathrm{LO}} &= 1.4653\ \mathrm{GeV}, & \Gamma_t^{\mathrm{NLO}} &= 1.3375\ \mathrm{GeV},\\
\Gamma_W^{\mathrm{LO}} &= 2.0481\ \mathrm{GeV}, & \Gamma_W^{\mathrm{NLO}} &= 2.1195\ \mathrm{GeV}.
\end{aligned} \tag{23}$$

The shown NLO results for the widths are computed with the renormalization scale $\mu = m_t$. We note that the use of

NLO expressions for the widths increases the NLO cross sections by about 10 percent.

We begin with the discussion of the Tevatron results. We consider $t\bar{t}$ production in the lepton + jets channel so that our leading order cross section contains five jets. The lepton transverse momentum and the missing energy in the event are required to satisfy $p_{\perp,l} > 20$ GeV and $E_{\perp}^{\rm miss} > 20$ GeV. Jets are defined according to the $k_{\perp}$-jet algorithm [43] with $\Delta R = 0.5$. The jet transverse momenta are required to be larger than $p_{\perp,j} > 20$ GeV. Both leptons and jets must be central $|y_l| < 2$, $|y_j| < 2$. To better discriminate against the background, we require an additional cut on the transverse energy in the event $H_{\perp} = \sum_j p_{\perp,j} + p_{\perp,e} + E_{\perp}^{\rm miss} > 220$ GeV. We present results below for a single lepton generation. Hadronic decays of W bosons to first two quark generations are included and the Cabibbo-Kobayashi-Maskawa matrix is set to the identity matrix.

The cross sections for $p\bar{p} \to bW^+(e^+\nu_e)\bar{b}W^-(jj) + j$ production at the Tevatron at leading and next-to-leading order in perturbative QCD, subject to the above cuts, read

$$\sigma_{\rm LO} = 75.29^{+49.2}_{-27.4}\ {\rm fb}, \qquad \sigma_{\rm NLO} = 78.9^{-5.6}_{-5.6}\ {\rm fb}. \tag{24}$$

In Eq. (24), the central value refers to renormalization and factorization scales set to $\mu = m_t$ and the upper (lower) value to $\mu = m_t/2$ and $\mu = 2m_t$, respectively. We observe a dramatic reduction in dependence on unphysical scales if NLO QCD corrections are included.

It is interesting to understand how jet radiation in the production and jet radiation in the decay contribute to cross sections shown in Eq. (24). To answer this question, we present separate cross sections for production and decay processes as well as mixed contributions, as defined in Eq. (3). For factorization and renormalization scales set to $\mu = m_t$ we find

$$\begin{aligned} \sigma_{\rm LO} &= 46.33\,({\rm Pr}) + 28.96\,({\rm Dec}) = 75.29\ {\rm fb}, \\ \sigma_{\rm NLO} &= 47.7\,({\rm Pr}) + 36.7\,({\rm Dec}) - 5.5\,({\rm Mix}) = 78.9\ {\rm fb}. \end{aligned} \tag{25}$$

This result is interesting because it shows that, with our choice of selection criteria, in only 60 percent of all events that contain a $t\bar{t}$ pair and a jet, the jet can be associated with the production process; in the remaining 40 percent of events, jets come from top quark decays. These fractions are stable against NLO QCD corrections, but the reason for that stability is peculiar. Indeed, it follows from Eq. (25) that the NLO QCD corrections to the production process are relatively small ($K = 1.03$) while QCD corrections to the decay process are quite large ($K = 1.37$). There is, however, a significant negative contribution from the "mixed" corrections. As described around Eq. (3), this contribution arises from single jet emission in the production convoluted with single jet emission in the decay and the corresponding virtual corrections. Because of this cancellation between decay and mixed contributions, a relatively small correction to jet radiation in top quark decays remains. Thus, an estimate of the NLO cross section that employs the exact leading order cross section as in Eq. (24) and the K factor for the production process $K = 1.03$ gives $\sigma_{\rm LO} \times K = 77.54$ fb, which is in good agreement with the full NLO result ($\mu = m_t$) in Eqs. (24) and (25). However, this cancellation seems accidental to us. In spite of the proximity of the two numbers for the $t\bar{t}j$ production at the Tevatron, we were unable to come up with a convincing and general argument that ensures that K factors for the production and decay processes are always similar. In fact, the importance of mixed and decay contributions strongly depends on the kinematic variables. For illustration we show production, decay, and mixed contributions as the function of the transverse momentum of the leading non-b jet in Fig. 2. At low $p_{\perp}^{\rm jet} \lesssim 60$ GeV, jet radiation in top quark decays is the largest ($\sim$60%) contribution to the cross section. As expected, at larger $p_{\perp}^{\rm jet}$, the jet is predominantly emitted in the $t\bar{t}$ production. The mixed contribution is positive at small jet momenta but changes sign at moderate $p_{\perp}^{\rm jet}$ and cancels the contribution due to jet radiation in decay at large $p_{\perp}^{\rm jet}$. The situation appears to be quite complex and observable-dependent. We can therefore anticipate—and we will see this explicitly in the context of the LHC discussion—that calculations without accounting for jet radiation in the decays of top quarks can lead to misleading results.

Various kinematic distributions at the Tevatron are shown in Figs. 3 and 4. For all kinematic distributions we find a significantly reduced dependence on the choice of the factorization and the renormalization scales as well as shape changes in kinematic tails of some distributions. The impact of QCD radiation in top quark decays is illustrated in the lower panes of each plot, where ratios of the full NLO cross section and the NLO $t\bar{t}j$ production cross

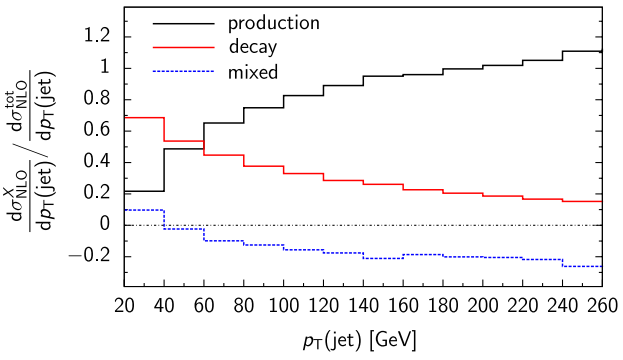

FIG. 2 (color online). Fractions of events when the leading (non-b) jet at the Tevatron comes from $t\bar{t}j$ production, the decay $t \to Wbj$, or mixed processes, as a function of jet transverse momentum. Note the sign of the mixed contribution and the cancellation between decay and mixed mechanisms at high transverse momentum. Renormalization and factorization scales are set to $\mu = m_t$.

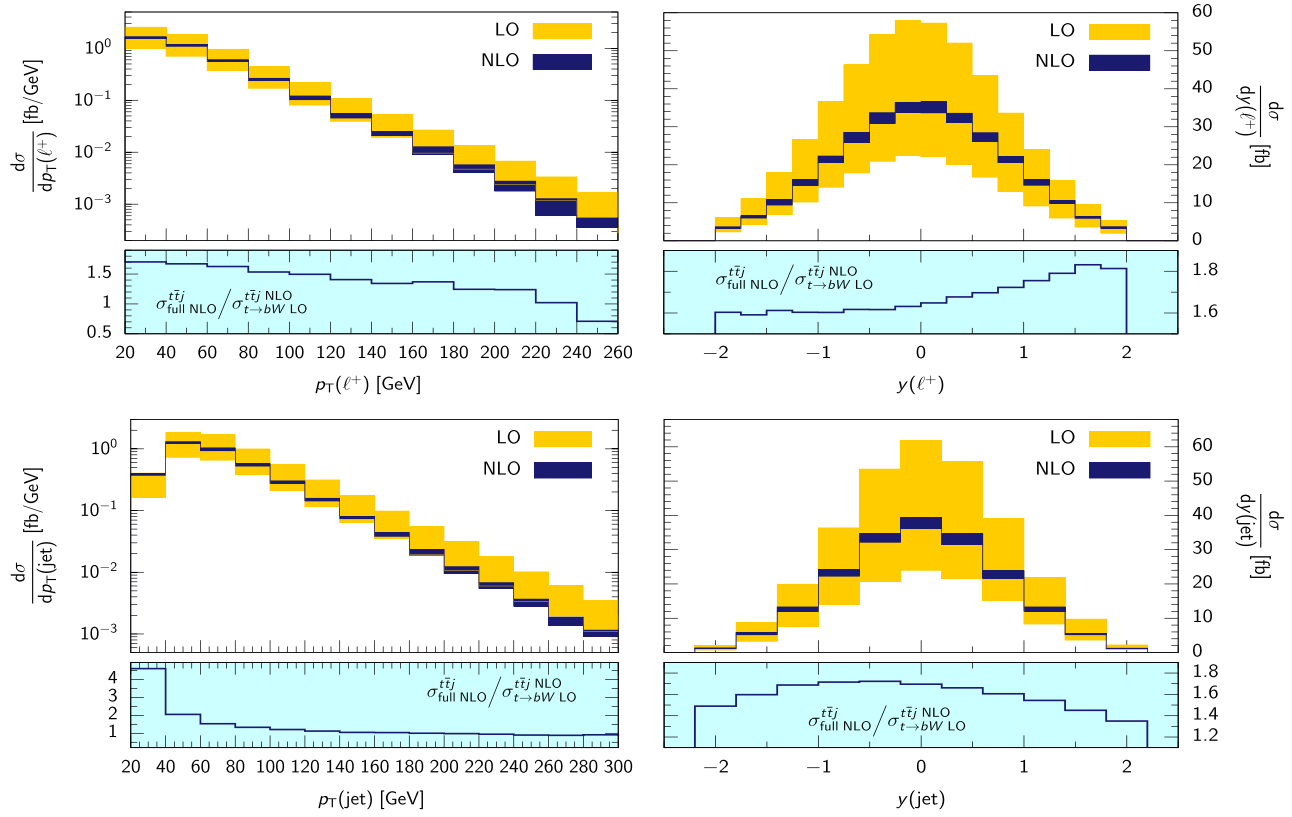

FIG. 3 (color online). Distributions of the lepton transverse momentum, the lepton rapidity, the transverse momentum, and the rapidity of the hardest jet for $t\bar{t}j$ production at the Tevatron at leading and next-to-leading order in perturbative QCD. The bands correspond to the variation of renormalization and factorization scales in the interval $m_t/2 < \mu < 2m_t$. Results with hard jet emission in the production stage only followed by leading order decays $t \to W + b$ are compared to full NLO results in lower panes.

section followed by the leading order decays of top quarks are shown. In general, these plots confirm the expectation that QCD radiation in top quark decays mostly affects spectra at low transverse momenta. But there are interesting exceptions where the impact of radiation in the decay is more pronounced. In particular, we find fairly uniform enhancement of transverse momenta and rapidity distributions of the charged lepton as well as the rapidity of the hardest jet (Fig. 3). The decay contribution to the rapidity distribution of a lepton is asymmetric; it appears to be more important at large positive rapidities. However, the full NLO distribution does not show significant asymmetry in lepton rapidity.

In Fig. 4 we show distributions of the transverse momentum and rapidity of the 5th hardest jet, the total transverse energy in the event $H_\perp$, and the transverse momentum of the $t\bar{t}$ pair. All these distributions receive nonuniform enhancements from jet radiation in top quark decays. In particular, $H_\perp$ and $p_\perp$ (5th jet) distributions are strongly enhanced at low values of $H_\perp$ and $p_\perp$, where relatively soft radiation in top quark decays dominates. Also, the rapidity distribution of the 5th hardest jet receives strong enhancement at central rapidities which is a consequence of the fact that top quark decay products are produced mostly at small rapidities. We note that similar shape changes were recently observed in the context of studying $p\bar{p} \to t\bar{t}j$ within the parton shower approximation in Ref. [27]. Note, however, that the cross section computed in Ref. [27] seems closer to the contribution that we identify as "jet radiation in production." While—as we just saw—such a result underestimates the cross section, it is probably consistent with the fact that decays in Ref. [27] are treated in the parton shower approximation which by construction conserves the overall probability and does not change normalization.

We also consider the distribution in the transverse momentum of the $t\bar{t}$ pair in Fig. 5. This kinematic distribution is particularly interesting because recent results by the D0 Collaboration [44] indicate a disagreement between predictions of MC@NLO [45] and data at low transverse momenta. Since we deal with top quark decay products rather than with stable top quarks, we need to define what is meant by the $t\bar{t}$ transverse momentum. To this end, we imagine that the reconstruction proceeds by finding two non-b jets whose invariant mass is closest to M_W and then combining the transverse momenta of these two jets, two b jets, the lepton transverse momentum, and the missing transverse momentum, to obtain the transverse momentum

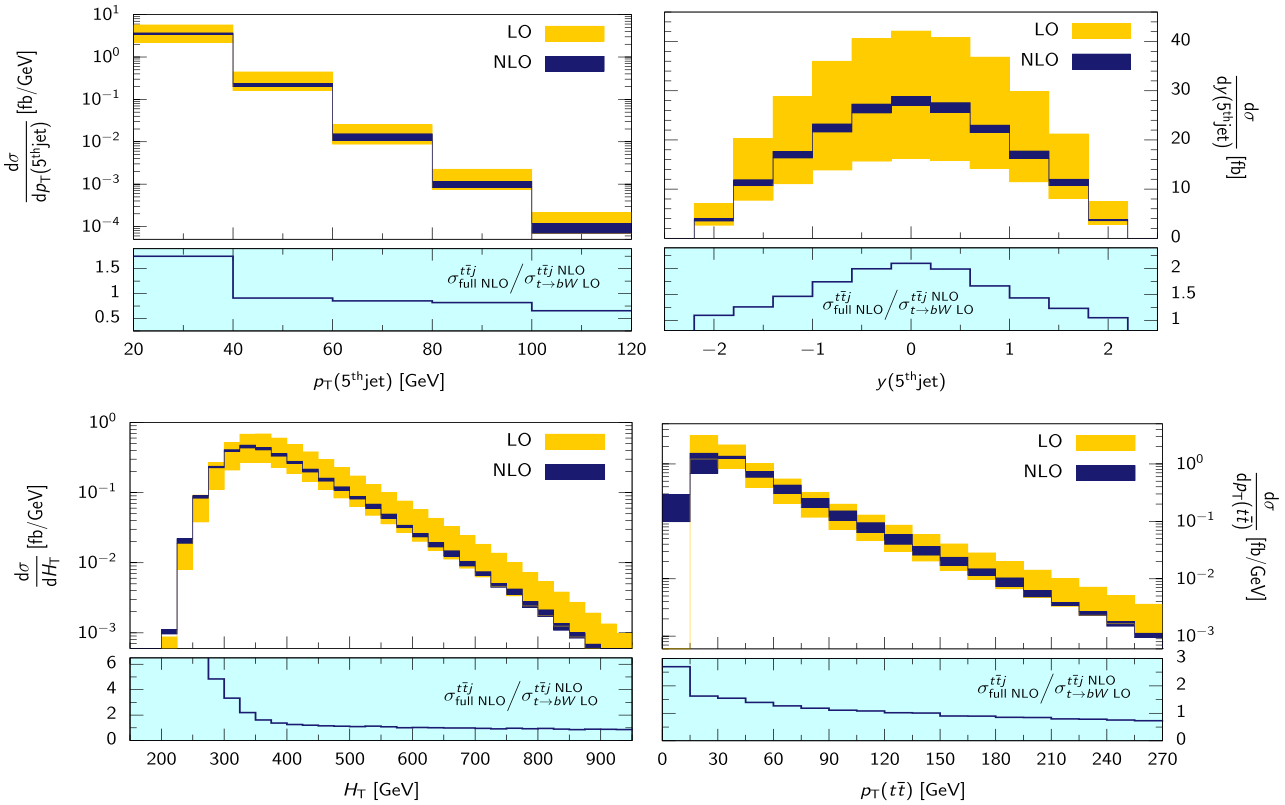

FIG. 4 (color online). Distributions of the transverse momentum and the rapidity of the 5th hardest jet, the transverse energy H_T, and the transverse momentum of the $t\bar{t}$ pair for $t\bar{t}j$ production at the Tevatron at leading and next-to-leading order in perturbative QCD. The bands correspond to the variation of renormalization and factorization scales in the interval $m_t/2 < \mu < 2m_t$. Results with hard jet emission in the production stage only followed by leading order decays $t \to W + b$ are compared to full NLO results in lower panes.

of the $t\bar{t}$ pair. We find that the transverse momentum distribution of the $t\bar{t}$ pair is affected by the radiation in the decay nonuniformly—the decay contributions are more important for small values of $p_\perp(t\bar{t})$.

To further match the results of our computation with the experimental setup in [44], we combine the $p\bar{p} \to t\bar{t}j$ calculation described above with a $p\bar{p} \to t\bar{t}$ computation at NLO QCD [22]. In the $p\bar{p} \to t\bar{t}$ computation we impose a jet veto prohibiting additional jets with the transverse momentum larger than 20 GeV, for consistency with the current $t\bar{t}j$ computation. We present our results[2] in Fig. 5. The normalization of the $\mu = m_t$ NLO computation is chosen such that the integral of the distribution is one. The lower pane in Fig. 5 shows that NLO QCD corrections to $pp \to t\bar{t}j$ and $pp \to t\bar{t}$ cause significant shape changes.

We continue with the discussion of $t\bar{t}j$ production at the $\sqrt{s} = 7$ TeV LHC. We imagine that W bosons from both t and $\bar{t}$ decays decay leptonically. For definiteness, we assume that the top quark decays to a positron and the antitop quark decays to an electron. All generic input parameters that we employ in the calculation were already described at the beginning of Sec. III. Specific to the LHC case, we require at least three jets, defined by the anti-$k_\perp$ jet algorithm [46] with $\Delta R = 0.4$. All jets have a minimum transverse momentum $p_{\perp,j} > 25$ GeV and central rapidities $|y_j| < 2.5$. Similarly, leptons need to satisfy

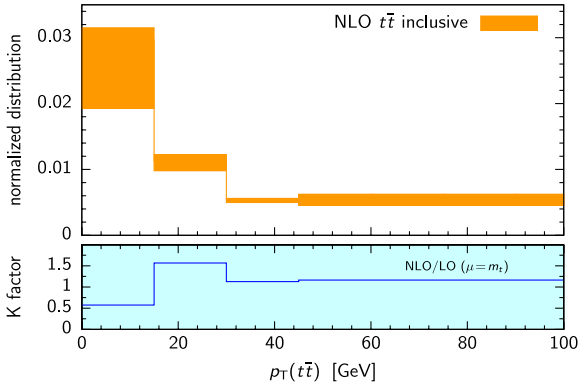

FIG. 5 (color online). Distribution of the transverse momentum distribution of the $t\bar{t}$ pair. The bands correspond to the variation of renormalization and factorization scales in the interval $m_t/2 < \mu < 2m_t$. The $\mu = m_t$ distribution is normalized in such a way that its integral equals to one.

[2]We note that the kinematic cuts on the final state particles that we use are similar but not identical to the ones used by the D0 Collaboration.

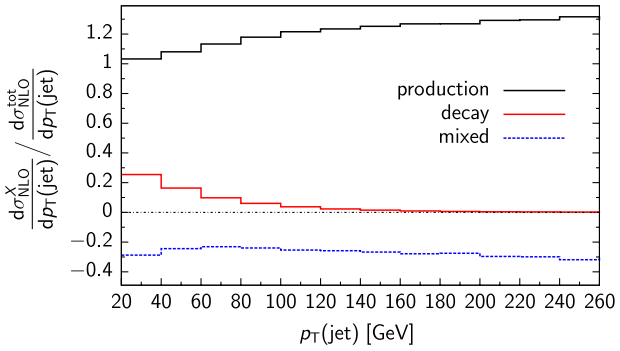

FIG. 6 (color online). Fractions of events when the leading (non-b) jet at the 7 TeV LHC comes from $t\bar{t}j$ production, the decay $t \to Wbj$, or mixed processes, as a function of jet transverse momentum. Note the sign of the mixed contribution and the cancellation between decay and mixed mechanisms at high transverse momentum. Renormalization and factorization scales are set to $\mu = m_t$.

$p_{\perp,l} > 25$ GeV and $|y_l| < 2.5$, and the missing energy in the event $p_\perp^{\text{miss}} > 50$ GeV. We find the following results for leading and next-to-leading order cross sections:

$$\sigma_{\text{LO}} = 350.3^{+215.0}_{-123.1}\ \text{fb}, \qquad \sigma_{\text{NLO}} = 288^{-46}_{-18}\ \text{fb}. \tag{26}$$

In Eq. (26), the central value refers to renormalization and factorization scales set to $\mu = m_t$ and the upper (lower) value to $\mu = m_t/2$ and $\mu = 2m_t$, respectively.

In case of the LHC, the interplay between radiation in the production and radiation in the decay is very different from the Tevatron. Since top quark pairs at the LHC are mostly produced in gluon annihilation and the collision energy is high, radiation in the production strongly dominates over radiation in the decay. We find ($\mu = m_t$)

$$\begin{aligned}\sigma_{\text{LO}} &= 316.9\,(\text{Pr}) + 33.4\,(\text{Dec}) = 350.3\ \text{fb},\\ \sigma_{\text{NLO}} &= 323\,(\text{Pr}) + 40.5\,(\text{Dec}) - 75.5\,(\text{Mix}) = 288\ \text{fb}.\end{aligned} \tag{27}$$

The three NLO contributions are shown in Fig. 6, as a function of the transverse momentum of the leading non-b jet. The radiation in the decay becomes less and less important as the process becomes harder, but the negative mixed contribution appears to be significant also at high $p_\perp$. Although radiation in the decay at the LHC is less important than at the Tevatron, it is peculiar that mixed contributions are large and negative.

We point out that this may cause misleading results, if the full (production and decay) leading order cross section and the next-to-leading K factor for the production process only are used to estimate the full NLO cross section. The K

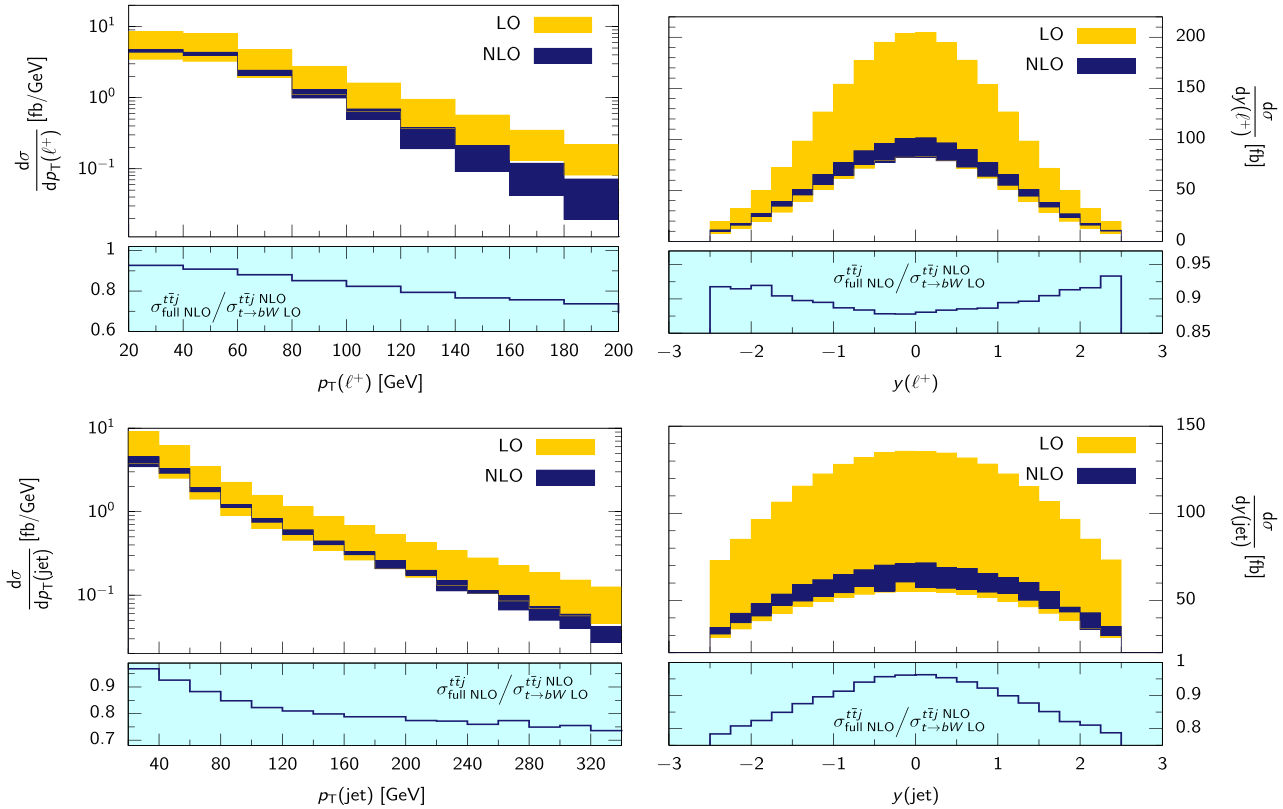

FIG. 7 (color online). Distributions of the lepton transverse momentum, the lepton rapidity, the transverse momentum, and the rapidity of the hardest jet for $t\bar{t}j$ production at the LHC (7 TeV) at leading and next-to-leading order in perturbative QCD. The bands correspond to the variation of renormalization and factorization scales in the interval $m_t/2 < \mu < 2m_t$. Results with hard jet emission in the production stage only followed by leading order decays $t \to W + b$ are compared to full NLO results in lower panes.

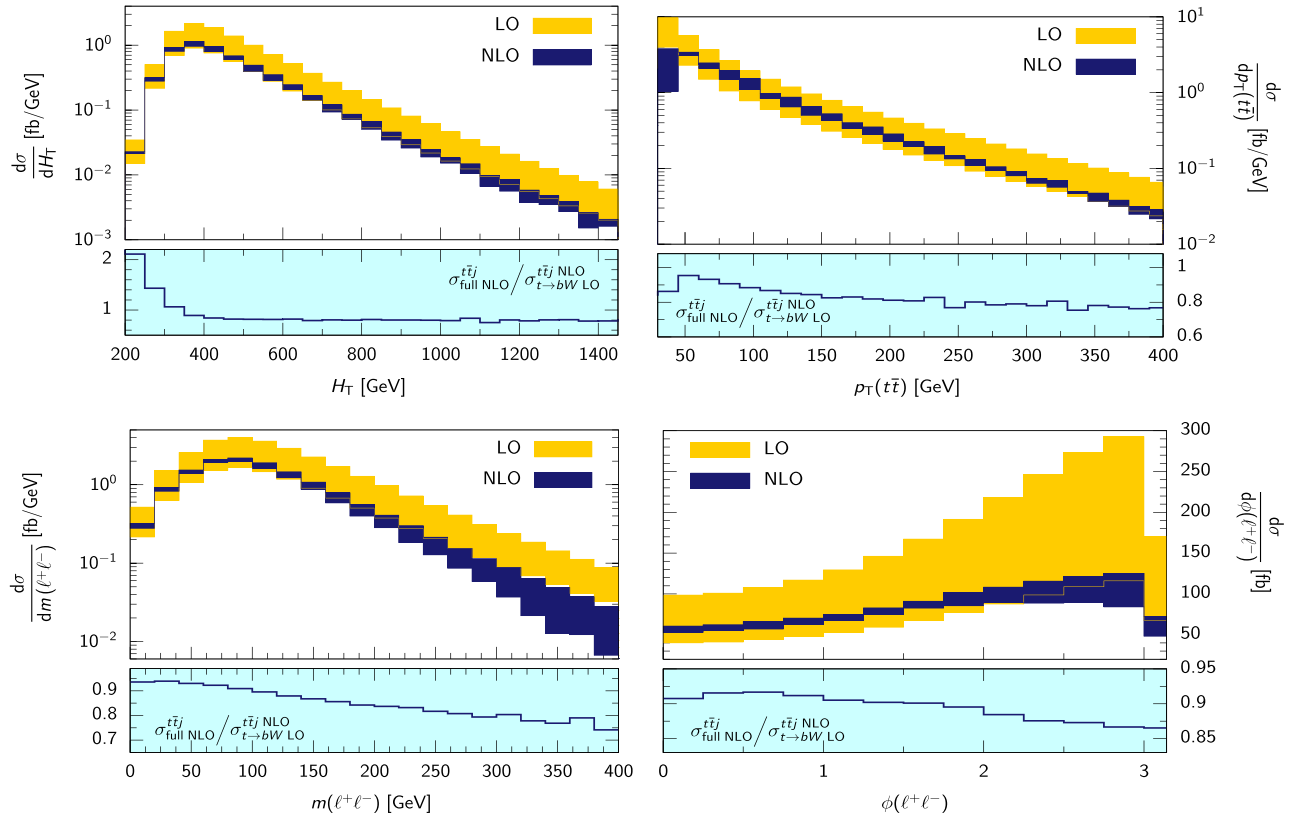

FIG. 8 (color online). Distributions of the transverse energy H_T, the transverse momentum of the top quark pair, the dilepton invariant mass, and the relative azimuthal angle between the leptons for $t\bar{t}j$ production at the LHC (7 TeV) at leading and next-to-leading order in perturbative QCD. The bands correspond to the variation of renormalization and factorization scales in the interval $m_t/2 < \mu < 2m_t$. Results with hard jet emission in the production stage only followed by leading order decays $t \to W + b$ are compared to full NLO results in lower panes.

factor ($\mu = m_t$) for the production process is 323 fb/316.9 fb ~ 1.02, so the naive estimate of the NLO cross section is $1.02 \times \sigma_{\text{LO}} \approx 357$ fb, which is about 20 percent higher than the correct NLO value given in Eq. (27). We emphasize that the mixed contribution to $t\bar{t}j$ production is a NLO QCD effect, so unless NLO effects are properly incorporated into computations of associated production of unstable particles, it is unclear to what extent various predictions for cross sections can be trusted.

In Figs. 7 and 8 we show various kinematic distributions for the LHC. The importance of QCD radiation in decays for various observables can be seen from the lower panes. We find that for the LHC the impact of the QCD radiation in the decay is modest; the variable that seems to be most affected is $H_\perp$ at small values of the transverse energy. For kinematic distributions in dilepton invariant mass or in the relative azimuthal angle of the two leptons, there is a uniform reduction, almost independent of $m_{l^+l^-}$ and $\phi_{l^+l^-}$. Finally, we note that given the discrepancy between the MC@NLO prediction for the transverse momentum of the $t\bar{t}$ pair and the D0 data [44], it is important to measure this distribution at the LHC. Thanks to a much higher energy and luminosity, the LHC should be able to probe a much broader distribution in $p_\perp(t\bar{t})$, including regions where fixed order QCD computations are directly applicable. We show the $p_\perp(t\bar{t})$ distribution in Fig. 8 and find that this distribution receives important modifications due to radiation in the decay.

IV. CONCLUSIONS

In this paper, we discussed the computation of NLO QCD corrections to the production of a $t\bar{t}$ pair in association with a hard jet at hadron colliders. While NLO QCD corrections to this process have been considered in the literature several times already, in this article for the first time, QCD radiative corrections to top quarks decays are studied, including the possibility that the jet is emitted in the decay stage. Within the narrow width approximation, the results reported in this paper lead to a complete and fully consistent treatment of top quark pair production and decay in association with a jet at next-to-leading order in perturbative QCD.

While at leading order there is a clear separation into production and decay stages, at next-to-leading order there appears a new contribution where one parton is emitted in

the production and the other parton in the decay. Since this mixed contribution must be supplemented by virtual corrections to ensure infra-red safety, we find that it can be negative. This leads to interesting effects that, to the best of our knowledge, have not been discussed in the literature before. In particular, it is far from clear that a widely used procedure is valid that estimates NLO QCD cross sections by computing leading order cross sections with decays and rescaling them by K factors obtained from calculations that ignore radiation of jets in the decay. In fact, we find that this procedure accidentally gives an accurate estimate of the NLO cross section for $t\bar{t}j$ production at the Tevatron but similarly overestimates the NLO QCD cross section at the LHC by 20 percent. The absence of clear pattern suggests that it is best to include QCD radiative corrections to decays of unstable particles into theoretical predictions for hard scattering processes.

Jet radiation in the decays can have significant impact on kinematic distributions. One such case is the $H_\perp$ distribution at the Tevatron which exhibits significant distortion due to radiation in the final state. While the situation at the LHC is less dramatic, even there certain distributions are systematically distorted at the 10 to 20 percent level.

Recent progress in NLO computations was driven by the idea that perturbative QCD can describe hard scattering well, pushing theorists towards providing realistic descriptions of complicated hard processes which can be directly compared to experimental data. Clearly, in the case of heavy short-lived particles such as top quarks, this implies that NLO QCD computations should be applied to their decay, including all spin correlations. All of this can be done in a rather straightforward way in the narrow width approximation which provides a parametric framework for such studies. We have demonstrated how this framework can be used to describe the production of $t\bar{t}$ pairs in association with a jet at hadron colliders. We look forward to further applying this framework for the description of both standard model and new physics processes at the LHC.

ACKNOWLEDGMENTS

We would like to thank R. Demina, A. Harel, D. Orbaker, and B. Webber for comments on the manuscript. This research is supported in part by NSF Grants No. PHY-0855365 and No. PHY-0547564, as well as by DOE Grant No. DE-AC02-06CD11357 and startup funds of Johns Hopkins University. Calculations reported in this paper were performed on the Homewood High Performance Cluster of Johns Hopkins University.

[1] T. Aaltonen *et al.* (CDF Collaboration), CDF Conf. Note 9850 (2009); see http://www-cdf.fnal.gov/physics/new/top/2009/xsection/ttj_4.1invfb/.
[2] T. Aaltonen *et al.* (CDF Collaboration), Phys. Rev. D **80**, 011102(R) (2009).
[3] A. Lazopoulos, T. McElmurry, K. Melnikov, and F. Petriello, Phys. Lett. B **666**, 62 (2008).
[4] A. Kardos, C. Papadopoulos, and Z. Trocsanyi, arXiv:1111.0610.
[5] M. V. Garzelli, A. Kardos, C. G. Papadopoulos, and Z. Trocsanyi, arXiv:1111.1444.
[6] R. Frederix, S. Frixione, V. Hirschi, F. Maltoni, R. Pittau, and P. Torrielli, Phys. Lett. B **701**, 427 (2011).
[7] S. Dawson, L. H. Orr, L. Reina, and D. Wackeroth, Phys. Rev. D **67**, 071503 (2003).
[8] W. Beenakker, S. Dittmaier, M. Kramer, B. Plumper, M. Spira, and P. M. Zerwas, Nucl. Phys. **B653**, 151 (2003).
[9] K. Melnikov, M. Schulze, and A. Scharf, Phys. Rev. D **83**, 074013 (2011).
[10] G. Bevilacqua, M. Czakon, C. G. Papadopoulos, and M. Worek, Phys. Rev. Lett. **104**, 162002 (2010).
[11] A. Bredenstein, A. Denner, S. Dittmaier, and S. Pozzorini, J. High Energy Phys. 03 (2010) 021.
[12] G. Bevilacqua, M. Czakon, C. G. Papadopoulos, R. Pittau, and M. Worek, J. High Energy Phys. 09 (2009) 109.
[13] T. Stelzer and W. F. Long, Comput. Phys. Commun. **81**, 357 (1994).
[14] A. Denner, S. Dittmaier, S. Kallweit, and S. Pozzorini, Phys. Rev. Lett. **106**, 052001 (2011).
[15] G. Bevilacqua, M. Czakon, A. van Hameren, C. G. Papadopoulos, and M. Worek, J. High Energy Phys. 02 (2011) 083.
[16] W. Bernreuther, A. Brandenburg, Z. G. Si, and P. Uwer, Phys. Lett. B **509**, 53 (2001).
[17] W. Bernreuther, A. Brandenburg, Z. G. Si, and P. Uwer, Phys. Rev. Lett. **87**, 242002 (2001).
[18] W. Bernreuther, A. Brandenburg, Z. G. Si, and P. Uwer, Int. J. Mod. Phys. A **18**, 1357 (2003).
[19] A. Brandenburg, Z. G. Si, and P. Uwer, Phys. Lett. B **539**, 235 (2002).
[20] W. Bernreuther, A. Brandenburg, Z. G. Si, and P. Uwer, Nucl. Phys. **B690**, 81 (2004).
[21] W. Bernreuther, A. Brandenburg, Z. G. Si, and P. Uwer, arXiv:hep-ph/0410197.
[22] K. Melnikov and M. Schulze, J. High Energy Phys. 08 (2009) 049.
[23] W. Bernreuther and Z.-G. Si, Nucl. Phys. **B837**, 90 (2010).
[24] S. Dittmaier, P. Uwer, and S. Weinzierl, Phys. Rev. Lett. **98**, 262002 (2007).
[25] S. Dittmaier, P. Uwer, and S. Weinzierl, Eur. Phys. J. C **59**, 625 (2008).
[26] K. Melnikov and M. Schulze, Nucl. Phys. **B840**, 129 (2010).

[27] A. Kardos, C. Papadopoulos, and Z. Trocsanyi, Phys. Lett. B **705**, 76 (2011).
[28] S. Alioli, S. Moch, and P. Uwer, arXiv:1110.5251.
[29] P. Nason, J. High Energy Phys. 11 (2004) 040.
[30] W. T. Giele, Z. Kunszt, and K. Melnikov, J. High Energy Phys. 04 (2008) 049.
[31] R. K. Ellis, W. T. Giele, Z. Kunszt, and K. Melnikov, Nucl. Phys. **B822**, 270 (2009).
[32] For a review see R. K. Ellis, Z. Kunszt, K. Melnikov, and G. Zanderighi, arXiv:1105.4319.
[33] S. Catani and M. H. Seymour, Nucl. Phys. **B485**, 291 (1997); **B510**, 503(E) (1998).
[34] S. Catani, S. Dittmaier, M. H. Seymour, and Z. Trocsanyi, Nucl. Phys. **B627**, 189 (2002).
[35] Z. Nagy, Phys. Rev. D **68**, 094002 (2003).
[36] J. M. Campbell and R. K. Ellis, Phys. Rev. D **62**, 114012 (2000). The MCFM program is publicly available from http://mcfm.fnal.gov.
[37] J. M. Campbell and F. Tramontano, Nucl. Phys. **B726**, 109 (2005).
[38] G. Passarino and M. Veltman, Nucl. Phys. **B160**, 151 (1979).
[39] R. K. Ellis and G. Zanderighi, J. High Energy Phys. 02 (2008) 002.
[40] J. M. Campbell, R. K. Ellis, and F. Tramontano, Phys. Rev. D **70**, 094012 (2004).
[41] Z. Bern and D. Kosower, Nucl. Phys. **B379**, 451 (1992); Z. Bern, A. De Freitas, L. J. Dixon, and H. L. Wong, Phys. Rev. D **66**, 085002 (2002).
[42] A. D. Martin, W. J. Stirling, R. S. Thorne, and G. Watt, Eur. Phys. J. C **63**, 189 (2009).
[43] S. Catani, Y. L. Dokshitzer, M. H. Seymour, and B. R. Webber, Nucl. Phys. **B406**, 187 (1993).
[44] V. M. Abazov *et al.* (D0 Collaboration), Phys. Rev. D **84**, 112005 (2011).
[45] S. Frixione and B. R. Webber, J. High Energy Phys. 06 (2002) 029; S. Frixione *et al.*, J. High Energy Phys. 08 (2003) 007.
[46] M. Cacciari, G. P. Salam, and G. Soyez, J. High Energy Phys. 04 (2008) 063.